Classification and reconstruction algorithms for the archaeological fragments

Nada A. Rasheed [a,*], Md Jan Nordin [b]

[a] University of Babylon, Hillah 51001, Iraq
[b] Universiti Kebangsaan Malaysia (UKM), Selangor 43600, Malaysia

ABSTRACT

The ancient pottery is often found in archaeological sites in a broken state, especially when those pieces of unknown organisms and irregular fragments, may take years of hard work, especially in the case of loss of some pieces or require hard work and experienced archaeologists. So this problem is divided into two major tasks the first of which is the Classification of Archaeological Fragments into similar groups (CAF) and the second one is the Reconstruction of each group into the original Archaeological Objects (RAO). To solve this problem, a method has been proposed, which exploits the color and texture properties of the surfaces of the fragments. Furthermore, the reconstruction of archaeological fragments in 3D geometry is an important problem in pattern recognition. Therefore, this research has implemented the algorithms to reconstruct real datasets using Neural Networks. The challenge of this work is to reconstruct the objects without previous knowledge about the part that should start the assembly; this greatly helps to avoid the presence of gaps created due to missing artifact fragments. The study utilizes the geometric features of the fragments as important features to reconstruct the objects by classifying their fragments using a Neural Network model.

© 2018 The Authors. Production and hosting by Elsevier B.V. on behalf of King Saud University. This is an open access article under the CC BY-NC-ND license (http://creativecommons.org/licenses/by-nc-nd/4.0/).

1. Introduction

An automatic reconstruction of ancient artifact fragments is a great interest in archaeology. It is considered important because it helps archaeologists access inferences about past cultures and civilizations Hristov and Agre (2013). Although variety algorithms have been proposed to reconstruct archaeological pottery fragments, few studies approached the classification of the fragments found in archaeological sites into similar groups Makridis and Daras (2012). In order to highlight the most important methods that the authors adopted over the past few decades for the classification of archaeological fragments in light of extracted features, most of the previous research was shown to rely on color feature Kampel and Sablatnig (2000), texture features Ying and Gang (2010), color and texture features Smith et al. (2010), Zhou et al. (2011), color and edges Makridis and Daras (2012), at last the profile, edge, color and texture Piccoli et al. (2013).

One of the main challenges is reconstructing the archaeological objects from a large number of fragments that are found in excavation sites Guoguang et al. (2016a), and determining the correct match between them Guoguang et al. (2018a). Occasionally, archaeological workers suffer when trying to match object fragments together, especially in the case of a presence of significant gaps in the fragments. Thus, numerous studies proposed methods for the purpose of reaching a suitable solution to reconstruct the archaeological 3D objects and returning them to their original forms such as Belenguer and Vidal (2012). Therefore, the main objectives of this work are listed as follows:

a) To propose a novel algorithm for classifying fragments depending on global and local features, specifically color and texture features, this be performed through proposed method that includes the intersection of color points of the images, and using the local binary patterns (LBP) feature that has proven to be more flexible with color feature, but requires more complex calculations.

* Corresponding author.
E-mail addresses: nadaar@siswa.ukm.edu.my (N.A. Rasheed), jan@ftsm.ukm.my (M.J. Nordin).

Peer review under responsibility of King Saud University.

Production and hosting by Elsevier

b) To design a robust prototype for the reconstruction of 3D objects, despite the existence of the gaps, by exploiting the geometric features (especially the slope of the edges of the fragments); as well as finding the appropriate location for matching.

2. Literature review

The idea of finding the possible solutions to the resemble of objects began as early as 1970, when Smith and Kristof (1970) were interested to reassemble the Egyptian Temple with computer assistance. Many studies have focused on the issue of archeology to find a solution based on two-dimensional images and three-dimensional model, whereas some of the researchers were interested in the proposed methods of classifying fragments into groups and reconstructing the archaeological objects. Smith et al. (2010) focused on the classification of two-dimensional fragments based on the properties of color and texture. While other authors deal with the problem on the basis of surface texture properties Ying and Gang (2010). Another type of studies (Makridis and Daras, 2012) had depended on the classification of the parts by using the technique the front and rear characteristics of the pottery to improve the classification accuracy and extract features based on color information and local texture. The study of Leitao and Stolfi (2005) focused on contour information for the reconstruction of ceramic fragments. Oxholm and Nishino (2011) reassemble thin artifacts of geometrically unknown through the photometric properties of the boundary contour.

Subsequently, most previous works focused on finding pairwise matches between adjacent fragments by using color surface which is one of the traditional features, that is why the work of authors Toler-Franklin et al. (2010) were so different from the others where have relied on a multiple-features that extracted from fragments based on color, shape and normal maps. Another work was suggested by Kimia and Aras (2010), which includes a framework or a practical system can be used by archaeologists to assembling 2D vessel fragment archaeological and that could be applied on the 3D fragments. By using the morphology profile, the authors Karasik and Smilansky (2011) were proposed a method that relies on the computerized morphological classification of ceramics. Oxholm and Nishino (2013) didn't adopt the shape of the object or its painted texture, but their work depended on similar geometry and photometry along, and across matching fragments adjoining regions. In the three-dimensional model case, much work has been done on the problem of automatically reconstructing fragmented objects. The authors Lu et al. (2007) provided an approach to reconstruct the fragments depended on boundary curves of the fragments and the interaction with archaeologists. Through a collaborative project Cohen et al. (2010) which considered as a formed a generic model based on the combined between the expert feedback to the archaeologist and vessel surface markings.

This model has been tested by using a ceramic artifact collection recovered from the National Constitution Center site in Independence National Historical Park. A method that classifies and reassembly of archaeological fragments based on the discriminating feature descriptors was proposed by Guoguang et al. (2016b), whereas Angelo et al. (2018) focused on analyses of pottery fragments by extracting 3D geometrical and morphological features. Then Precision and durability have emerged in the work of continuous fragments in the dimensional analysis of certain recognized properties.

3. Materials and methods

This paper presents a proposed framework to solve the problem of classification and reconstruction of archaeological fragments.

The proposed methodology consists of two phases; each one performs a specific job, as shown in Fig. 1a.

The framework of the system in Fig. 1b consists of two parts, Classification of Ancient Fragments (CAF), and Reconstruction of Ancient Objects (RAO). Each framework consists of a set of procedure, as shown in the following steps:

(a) Standard image acquisition from the website.
(b) Object segmentation.
(c) Feature extraction depending on color and texture of the surfaces of the fragments and the globule and locale features.
(d) Classify fragments into groups; if it is no part of the collection, it must be returned to the dataset for re-entry so that it is suitable for grouping with other parts. However, in the case that all parts formed the group, they are moved to the next stage, which is to reconstruct the group into a single object.

The second stage involves

(a) Acquisition 3D model and apply the preprocessing procedure to eliminate the noise that appears as the result of scan object, and then calculate the geometric features after extracting the contour of each part and divided into subsets.
(b) Identify the part that will match a pair of fragments by using Neural Network.
(c) Aligning the candidate 3D fragments and matching through proposed new method. If the object no complete should be brought back to the dataset. Otherwise, the procedure is finished, and the object was obtained a fully.

3.1. Classifying fragments into groups

The framework of classifying fragments into groups consists of a set of procedures as shown in Fig. 1b, which can be summarized in the following steps:

a) Image acquisition.
b) Object segmentation.
c) Feature extraction depending on color and texture of the surfaces of the fragments and fragments classification into groups; if the fragment does not belong to the group, it should be brought back to the dataset to re-input it until being suitable for grouping with other fragments.
d) When all fragments have formed a group, the next stage starts, i.e. reconstructing the group into one object.

After the system has run, six images of fragments files will have been loaded into the memory directly. These images were captured using a Nikon camera, as shown in Fig. 2a.

In order to obtain the fragments without a background, we depended on the algorithm which is similar to the one used in Rasheed and Nados (2018) whose content is as depicted in Fig. 2b and when the algorithm begins to work, the result will be as set out in Fig. 2c.

In order to obtain the features of each fragment, this work depends on the color by calculating the colors intersection for each pair of fragments. Therefore, to extract the RGB color, we rely on the mathematical method which is similar to the one used in Rasheed and Nordin (2015), and includes the intersection of RGB matrices between each image with the corresponding of the other images. The algorithm is as follows Rasheed and Nordin (2015):
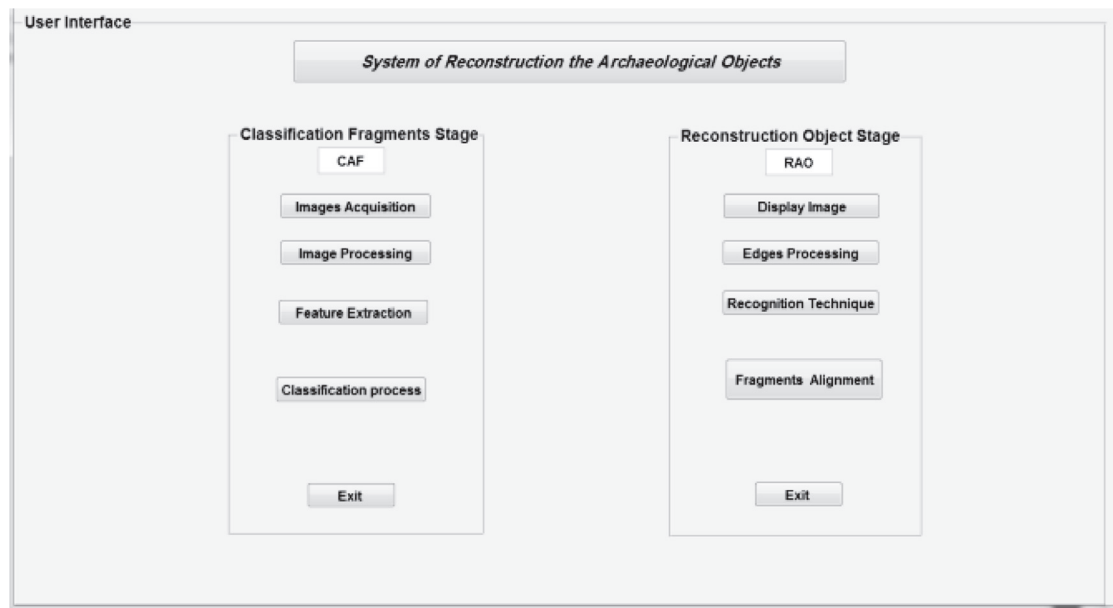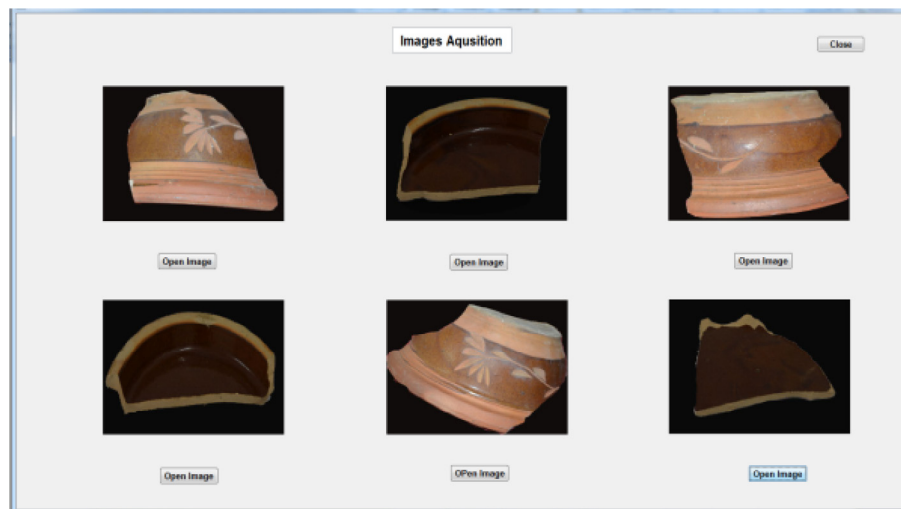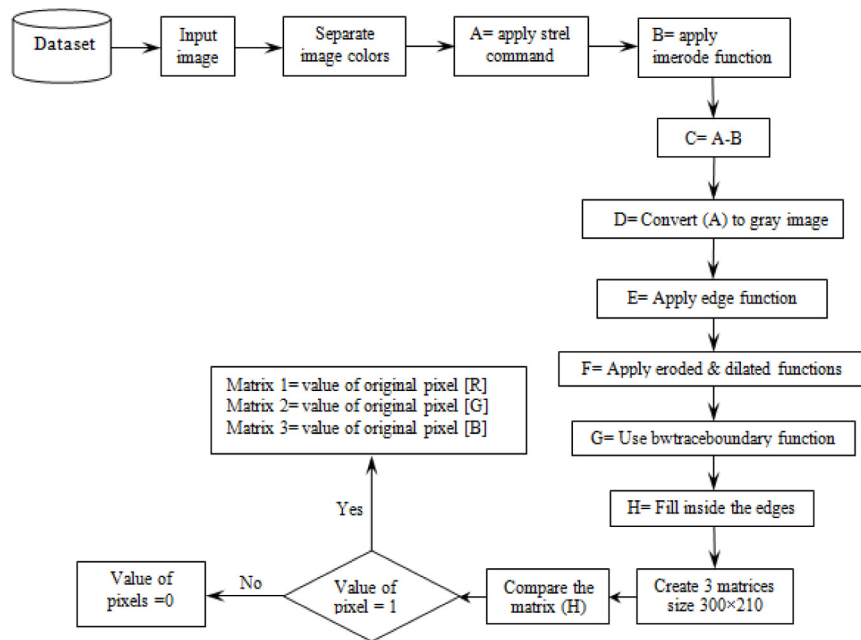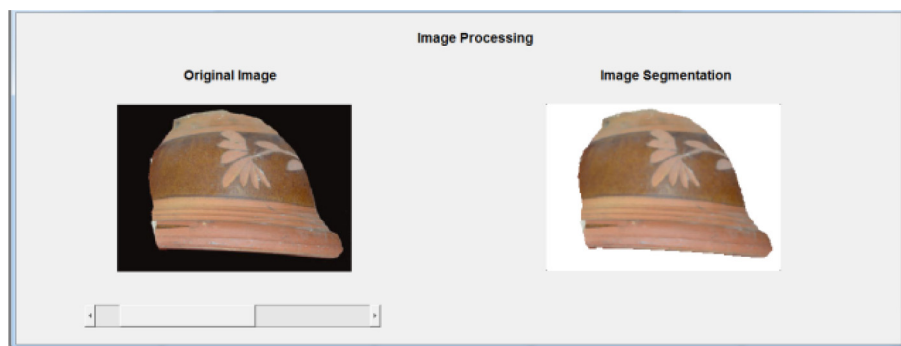
a
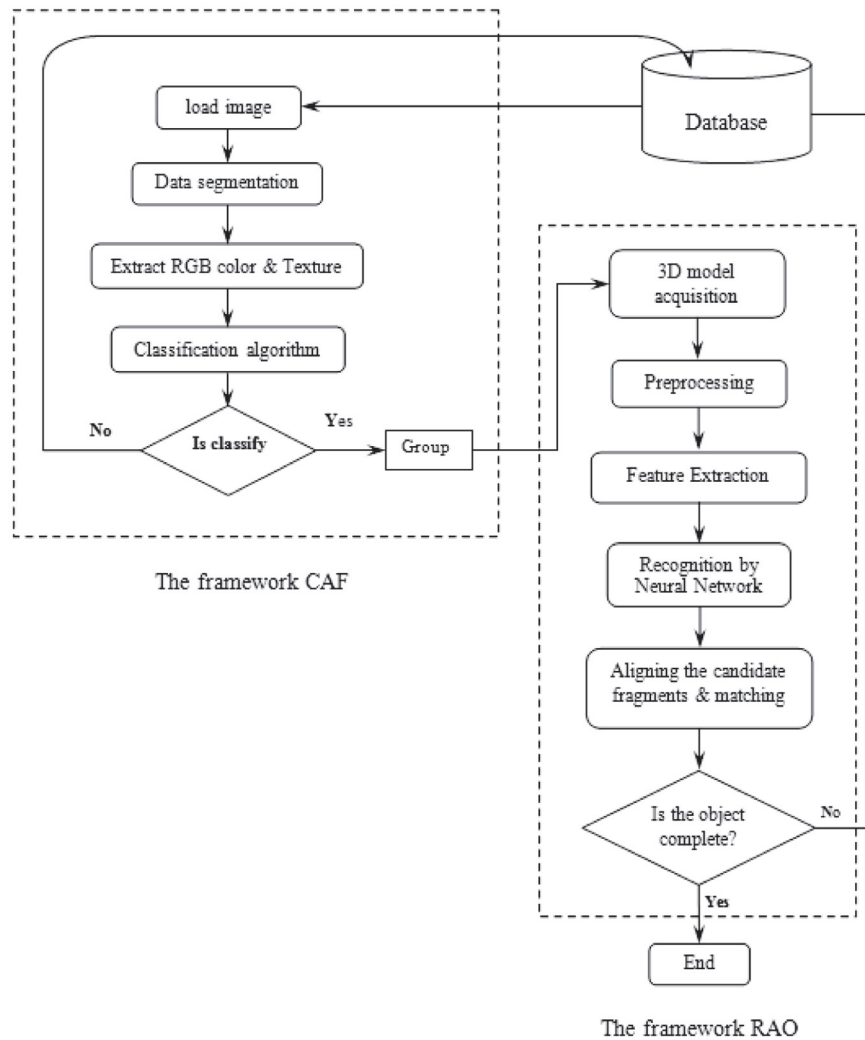
b

Fig. 1. Represents a) The interface of the system. b) The framework of the system.

a

b

c

Fig. 2. a) Upload images to the memory. b) Diagram of Image Segmentation (Rasheed and Nados 2018). c) Represents the result of Image Segmentation.

Step 1: Determine the values of the three colors in each pixel.
Step 2: For each image, all the surface points are stored in an array which is obtained as a set of values arranged in a parallel manner.

$$C = \{\forall P(Red_{ij}, Green_{ij}, Blue_{ij})\}$$

where $i = 1 \dots n$, $j = 1 \dots m$ and (n, m) are the dimensions of the image matrix.

Step 3: A is a set, each element consist of three values [Red, Green, Blue] regarding the first image. Similarly, B is a set each element represents three variables regarding to the second image.

$$A = \{\forall P_1(Red_{ij}, Green_{ij}, Blue_{ij})\}$$
$$B = \{\forall P_2(Red_{ij}, Green_{ij}, Blue_{ij})\}$$

where P_1 and P_2 denotes the number of the color elements in the set A (first image), and set B (second image) respectively.

Step 4: Obtain the set S, which represents the results from the intersection of colors between the two images:

$$S = A \cap B$$

Step 5: This procedure is repeated for another two images, until we obtain all intersections between all images, each element of each set is a vector representing the values of three colors.

As shown in Fig. 3a, this demonstrates the results of classification before applying the classification procedure. The graph shows the first image achieving the highest value of colors intersecting (8110, 8411) with the third and fifth images respectively, so the three images will be the first group. Also, the second image achieves the highest intersection (2724, 1783) with the fourth and sixth images respectively; these images also will represent the second group.

Many researchers consider the texture of objects or regions is an important feature used to recognize Haralick et al. (1973). Thus, this work exploits this feature by utilizing the Local Binary Patterns (LBP) Ojala et al. (1996). This method was suggested by Ojala et al. in 1996 to describe the texture of an image as a vector that labels the pixels on it into histogram describing a small-scale appearance of the image, thus using it for further image analysis Pietikäinen et al. (2011). So, the result of the first fragment is as shown in Fig. 3b and c.

The classification operation is divided into two steps: the first step classifies the fragments depending on the color using the proposed algorithm Rasheed and Nordin (2015), on the basis that there are two fragments as shown in Fig. 4.

Step 1: $R = $ [Color feature for first image,. . .. . .., Color feature for sixth image].
Step 2: Sort Ascending order for color feature of first image A.
Step 3: Compare the max value in the first column feature of image A with intersect values of image B.
IF the value of B is the highest value
    Group and saved A with B.
else if the value of $B > A$
    Compare the max value of the B with max value of the image that achieved a highest intersect C:
IF max value of the C; Do not group A with B
    else; Group A with B and saved the result.
Step 3.1: Moved to the second highest value, which represents the intersection with the other image.
Step 3.2: Repeat this procedure.
Step 3.3: Return to the first step until all the values in the first
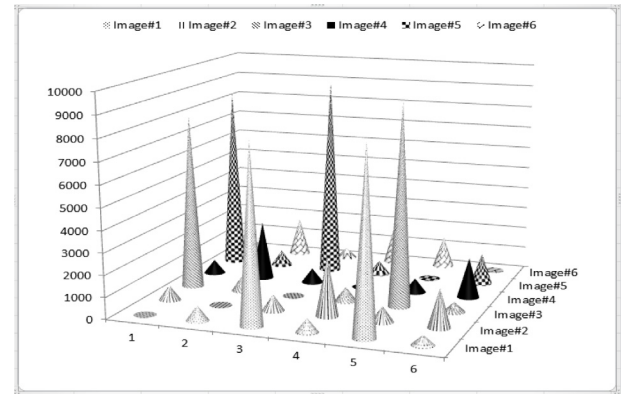
a
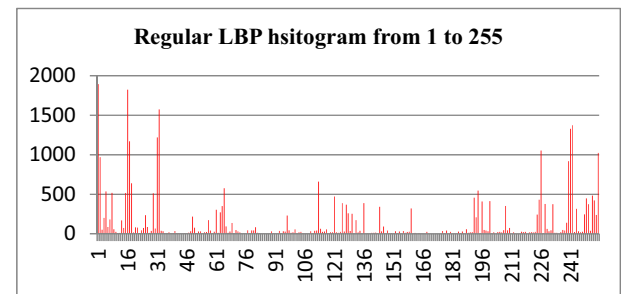
b
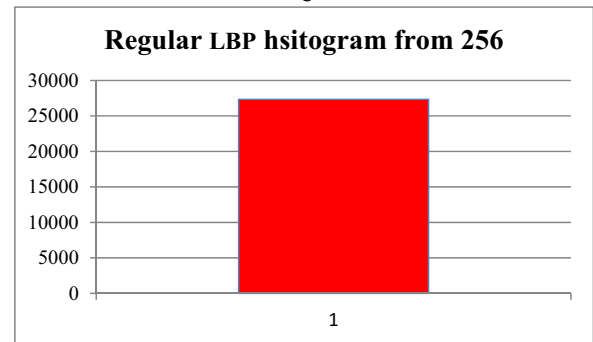
c

Fig. 3. a) The intersection between six color images. b & c) Histograms of LBP for the first fragment.

Fig. 4. Two parts of a broken object.

column finished.
Step 4: Repeat the procedure until all columns represents rest the images are complete.

The second step classifies the fragments based on the texture using the Euclidean distance. Thus, the final result will be manifest when the results of classification of color and texture are identical. There-

fore, the results should be saved for the next step – in this example only the second and third groups are saved.

3.2. Reconstructing each group into 3D object

Using Three-Dimensional measurements to resolve the problem of the reconstruction of archaeological artifacts has become widespread Guoguang et al. (2018b). Occasionally, archaeological workers suffer when trying to reassemble each group of ceramic into the object with high accuracy, especially if there is a presence of significant gaps in the object, or even when the fragments of the object are so many. The main theme of this part is to propose a system for the reconstruction of ancient 3D objects to the original form. The challenge of this work is to assemble the objects without previous knowledge of the part that must start in the compilation and this helps a lot to avoid the presence of gaps during losing parts of the artifacts.

For the purpose of reconstructing the pottery fragments, this work proposes a method that consists of four major phases as shown in Fig. 5.

3.2.1. Acquisition of 3D model

In order to reconstruct the real datasets, this work obtained 3D models of objects via the 3D laser scanner Primesense Carmine 1.09 3D scanner device. The datasets consist of two vessels, each one comprised of 3 fragments, as shown in Fig. 6a.

After classifying fragments into groups has finished, the algorithm of reconstructing each group starts by loading 3D models of fragment files in the memory. A single group will be selected in reconstruction window, which represents one vessel.

3.2.2. Feature extraction

Considered to be better than 2D, 3D features are used for recognition, but it may be more expensive. Axiomatically, when the archaeologists attempt to re-assemble the broken pieces, the assembly will be through the edges of the fragments which means extracting the geometric features. After that, they will check the texture and color of the surfaces of the fragments. Thus, in order to extract the features, this paper utilizes the edges of the fragments as an important feature to reconstruct the objects, so the following algorithm represents this procedure and the results as shown in Fig. 6b:

Step 1: Find all edges in the mesh, note that the internal edges are repeated.
Step 2: Determine uniqueness of edges.
Step 3: Determine the counts for each unique edge.
Step 4: Extract edges that only occurred once.
Step 5: Plot the edges.

The aim of this paper is to locate the correct location for matching two fragments and to continue matching the rest of the parts, as shown in Fig. 6c. It shows the similarity at the beginning of the slopes of the sub-contours A and B, and continues with the rest of sub-contours.

In order to locate the correct position, we decided to divide the contour of the fragment to four-parts of equal size as much as possible, and handle each part as a separate object, so for this fragment each part consists of 75, 75,75, and 72 points, as shown in Fig. 6d.

Then every part is divided into the sub-contours each of which consists of five points, to consequently have 59 sub-contours for current fragment, two remaining points being neglected. Taking the measure of the slope for each sub contour into account is the main characteristic to distinguish the place that should be matching a pair of different parts for two different fragments. Therefore, what was applied is the algorithm found in Maidment and Tarboton (2011) of 3D slope on each part and the result as demonstrated in Fig. 7a.

Other features extracted in this work are based on the all coordinates of each point (x, y, z) to calculate the minimum point for each sub-contour on the axes x, y, z and similarly the maximum, mean, and the variance values between the points of the sub contour for four parts are calculated. Results are shown in Fig. 7(b, c, d and e).

Thus, we will have thirteen features for each sub-contour which can possibly be used for entering a pair of fragments of matching. For the other two pieces as shown in Fig. 8a, it is obvious that fragment (B) consists of 55 sub-contours with three points being neglected, while the fragment (C) consists of 59 sub-contours with four points being neglected. Therefore, after extracting feature vectors, a matrix (13×114) will be ready to be the input of the network. Note that before training a neural network, the input must be normalized.

The next step, a procedure has been applied to detect the joint between the pair of sub-contours according to the similarity features, this work used the Backpropagation algorithm, which is a powerful mapping network that has been applied successfully to a wide variety of problems Duda et al. (2001). Hence, the structure of the neural network is composed of three layers; the first layer consists of 13 nodes of input; the second one - namely the hidden layer- consists of 30 nodes found through the experience; finally, the target output layer consists of 8 units, because this layer assigned one node for each part of the fragments $(B$ and $C)$, so the test data will be in the range of $(1, -1)$ Beale et al. (2015). In order to increase the network effectiveness and make it more suitable, the learning rate (0.05) with momentum term (0.9) was used. After training the neural network, it is worth mentioning that it is completed in 335 iterations of 1000 epochs that we assumed.

As shown in Fig. 8b, in order to recognize the unknown part of the fragment (A) to match it with the corresponding parts of the other fragments, we used the features of each part mentioned separately in Fig. 7 (b, c, d and e) to be unknown into the input layer of the network and test it through the Feed-forward phase.

After testing each part of the fragment (A), the results are as shown in Fig. 9(a, b, c and d).

Subsequently, after computing the actual output, the part of the fragment is a winner if the maximum value between the computed output nodes is close to one. Hence, it can be seen that the first part of the fragment A can match the corresponding one of the sixth part of the second fragment, because the red line achieves the highest values among eight nodes; so the assembly begins from the third sub-contour and continues to the end of the part. Here, what is adopted is the maximum value among eight nodes because we have assigned 1 to the current part and zeros otherwise. Immediately after recognizing the pairs of sub-contour between the edges of fragments A and B which probably represent the same point in space, aligning and matching should be started. This is often done simply by matching each point with its closest neighbor of the other cloud. In this case, the angle of rotation and the distance of transition between the two fragments must be computed. Fig. 10a shows an example of that.

Thus, this research suggests one algorithm for matching two edges of different parts of fragments. Suppose we have two fragments (A) and (B), fragment (A) should be fixed and fragment (B)

Fig. 5. The diagram of the proposed method to reconstruct the 3D object.
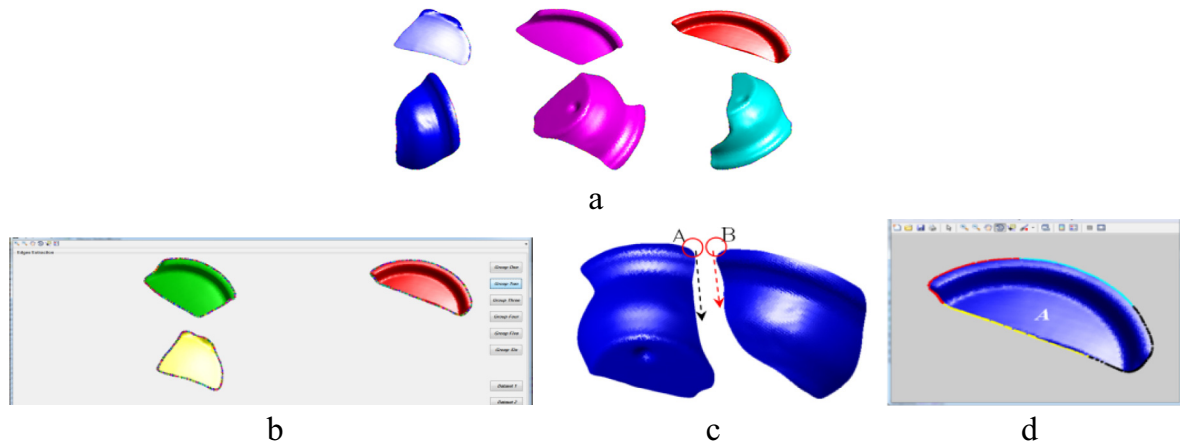
Fig. 6. Illustration a) Two groups of 3D fragments. b) Boundaries of three fragments. c) Recognize the matching place. d) Divides contour into four equal-sized.
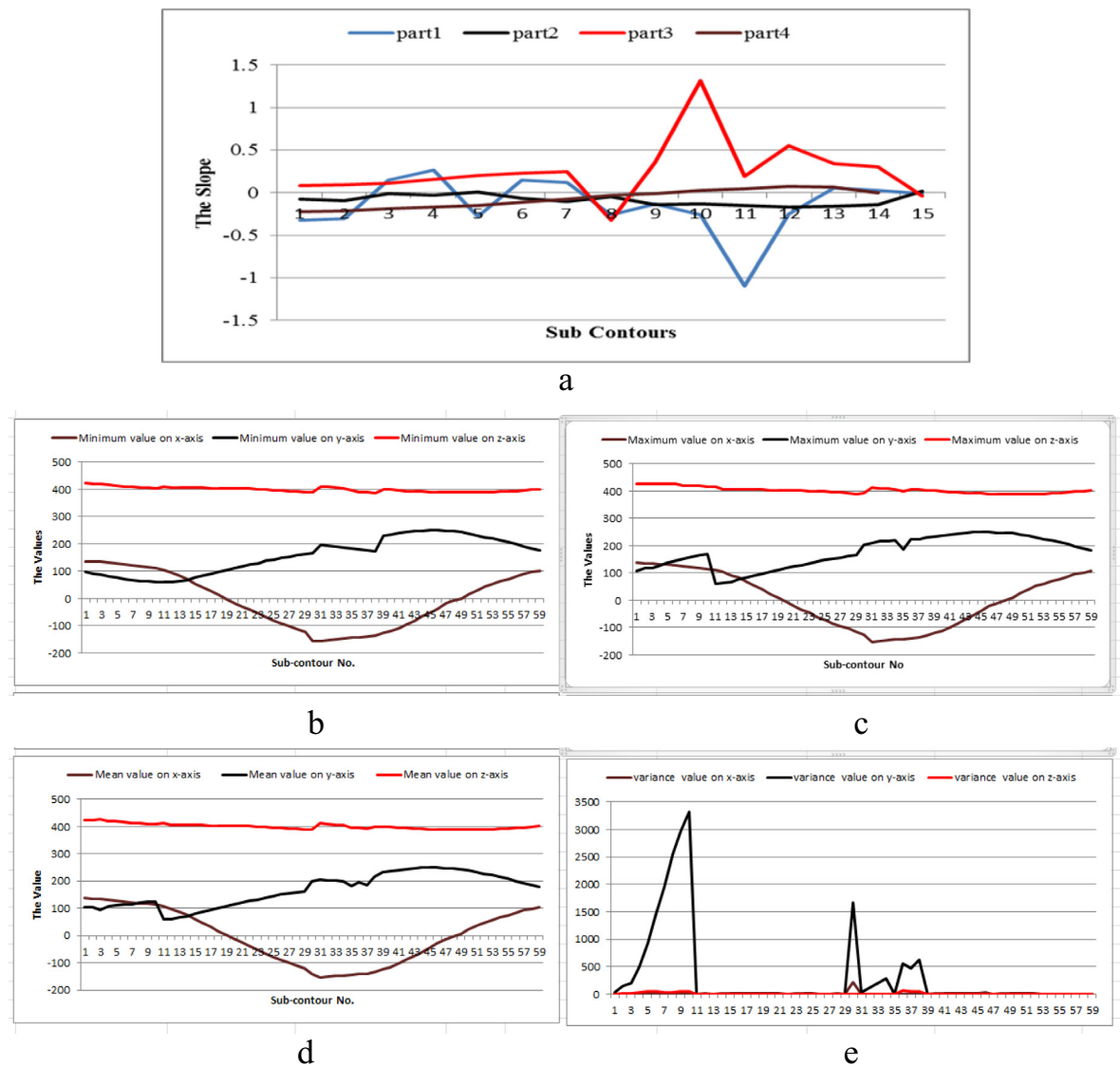

Fig. 7. For Each sub-contour a) The slopes b) Minimum Values c) Maximum Values d) Mean Values e) Variance Values.
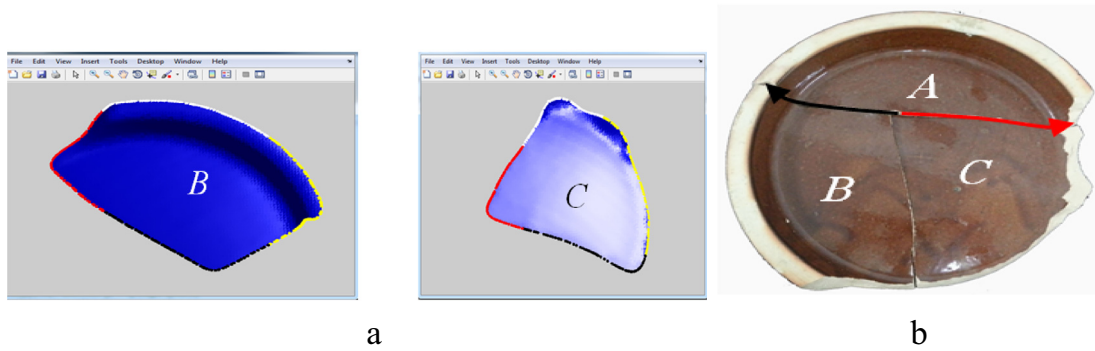
Fig. 8. a) Two Fragments That Divided into Four Parts. b) Represent Broken vessel.

should be followed. So in order to centralize the fragment (A) data at the zero, the following steps must be done:

Step 1: Find the center of fragment A:

$$p = \begin{bmatrix} x \\ y \\ z \end{bmatrix};$$

where the xyz data of fragment (A)

$$Center_A = \frac{1}{N} \sum_{i}^{N} p_N^i;$$

Step 2: Accumulating matrix (H)

$$H = \sum_{i=1}^{N} (p_A^i - Center_A);$$

Step 3: Using Singular Value Decomposition (SVD) to find the direction of most variance, and rotate the data to make it the x- axis as follows

$$[U, S, V] = svd(H, 0);$$

where U is $m \times n$ and column orthogonal (its columns are eigenvectors of AAT); V is $n \times n$ and orthogonal; D is $n \times n$ diagonal (non-negative real values called singular values). If H is $m \times n$ and m greater than n, then SVD computes only the first n columns of U and S is $n \times n$.

$$R = V \times U^T;$$

V is the direction of the most Variance

Step 4: Slide the data up the x- axis so all the points are $x \geq 0$.

$$T = -R \times Center_A;$$

After fixing fragment (a) to the origin points, optimal rotation (matrix R) should be found apart from translating (T) to the fragment (b).

Applying the experiments with 3D alignment method which seems to be is a difficult task for many authors Sui and Willis (2008), because it is necessary to identify the angle that should rotate the fragment surface (b) according to the x, y, and z-axes. Therefore, in order to achieve the best fit alignment, the Dot Product Nitecki (2012) was applied to find the angle on which the

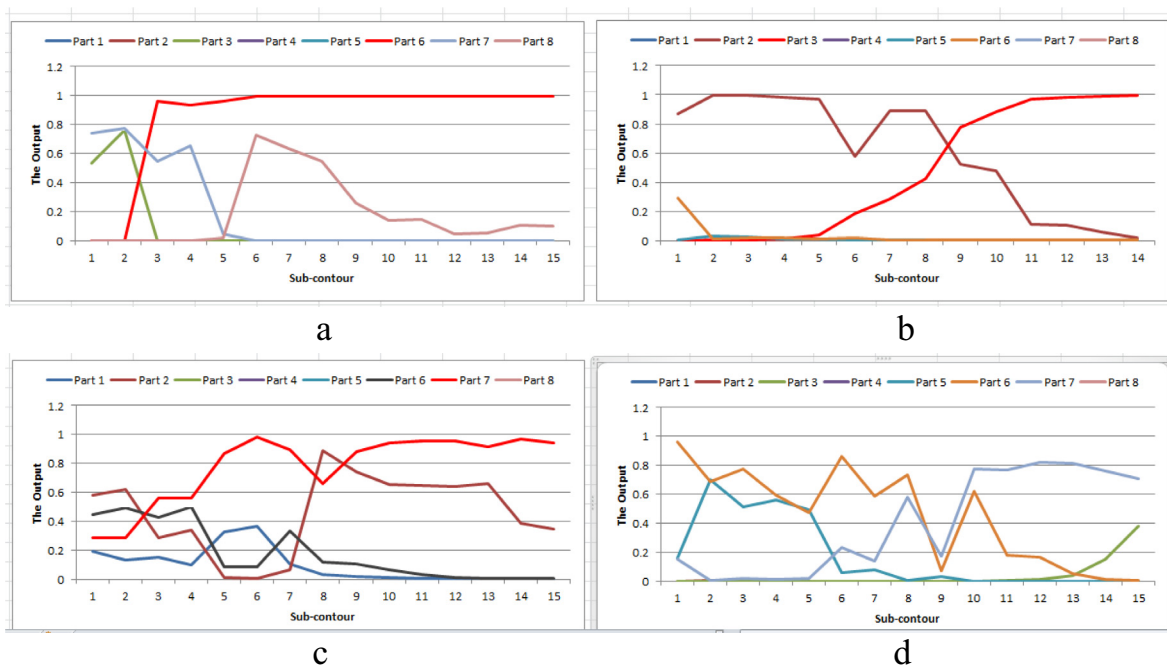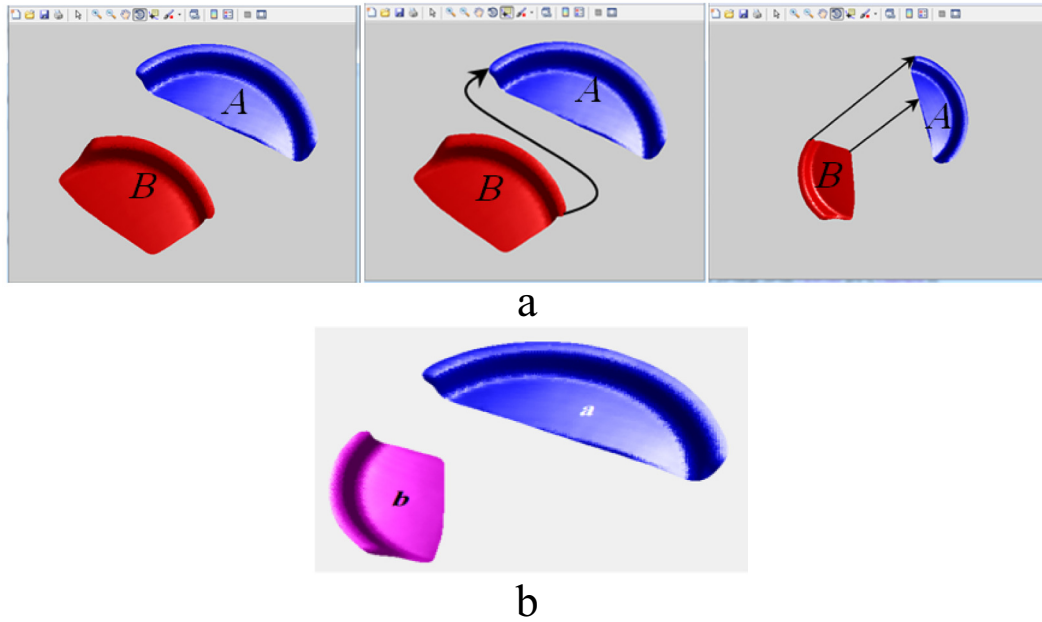**Fig. 9.** The test to the Fragment A: a) Part 1 b) Part 2 c) Part 3 d) Part 4.

a

b

Fig. 10. a) Two fragments should rotate and transform. b) Fragments *b* rotates to the fragment *a*.

fragment (*b*) must be rotated. In this case, the angle was returned inverse cosine ($\cos^{-1}$) of the elements of *θ* in degrees. Therefore, the object can be rotated around *x*, *y*, and *z*- axes Sui and Willis (2008) – through a number of experiments, the best result can be achieved by means of rotating the fragment around the *z*- axis according to the following formula:

$$Rz = [\cos(\theta) - \sin(\theta)0; \sin(\theta)\cos(\theta)0; 0\,0\,1] \tag{1}$$

In order to provide a solution to rotate the object, the equation (2) is proposed.

$$C = P_B \times R_z; \tag{2}$$

where *C* is the new 3D point cloud, P_B is the oldest 3D point cloud, and R_z is the rotation matrices. As shown in Fig. 10b the best rotation is around *z*-axis, so this research depended on this type. The other issue is to add a difference distance between the two objects' coordinates for the purpose of transfer (*T*) the object and matching the two sides of the pair various objects.

One of the fragments should be submitted to a transformational algorithm in order to bring it close to the other and to achieve the best fit alignment. Therefore, in order to provide a solution for *R* and *T* as in the equation (3), suppose *b* is the 3D point cloud data of the followed fragment:

$$C = P_B \times R_z + T; \tag{3}$$

where $T = (x + t_x), (y + t_y), (z + t_z)$, and *t* represent difference distance between the two objects; *R* and *T* rotation and transformation have been applied to 3D point cloud (*b*) to align it with 3D point cloud (*a*), as best as possible.

Finally, in order to obtain the optimal matching, the Euclidean distance formula has been applied between the coordinate of each point on the edge of the fragment (*b*) and all point coordinates of the corresponding fragment, followed by choosing the shortest distance. Given two points (*a*) and (*b*), the Euclidean distance is:

$$d(a,b) = \sqrt{(a_x - b_x)^2 + (a_y - b_y)^2 + (a_z - b_z)^2} \tag{4}$$

Given a point *b*, and set of points *A*, the Euclidean distance is:

$$d(b,A) = \min_{i \in 1.....n} d(b,a_i); \tag{5}$$

where *b*, a_i indicates the values of the points representing two sub-contours already classified as (*A*) and (*B*); *n* is the vector size. The last step is to slide the data up the *z*- axis, so all the points will be positive. The algorithm has been tested on several models of fragments, and it has achieved highly precise results in reconstructing the objects to the original forms, even in the cases when pieces were missing.

4. Compare the method with the other methods

4.1. Classifying fragments into groups

In order to evaluate the performance of the proposed framework CAF on the ceramic fragments database, several experiments have been conducted using the dataset obtained from the website (Ceramic Sherd Database, 2010) Makridis and Daras (2012). Totally, eighty artifact fragments used by Smith et al. (2010), having applied the Scale Invariant Features Transform (SIFT) and Total Variation Geometry (TVG) methods which rely on color and texture features to classify the ceramic fragments. They have achieved 76% by using SIFT and 75% by using TVG as depicted in Table 1, whereas the CAF system has achieved 96.1% using the method of intersection of RGB colors and LBP. This means the proposed method achieved a success rate higher than previous studies when applying the same test dataset.

Therefore, the technique used of colors intersection has played an important role in identifying fragments that symmetric in colors. Moreover, the proposed classification process provides highly accurate results.

4.2. Reconstructing each group into 3D object

In order to evaluate the performance of the proposed framework RAO, the authors Willis and Cooper (2006) were presented a method able to reconstruct the relics consisting of four fragments out of seven back to Nabatean Drinking Vessels Willis and Cooper

(2008). This artifact dating back to approximately 400B.C, which excavated from Petra, Jordan Sui and Willis (2008). Their approach includes estimating the global shape of the pot depending on the measurements of its fragments such as 2D profile curve and 3D line (the axis of symmetry), as shown in Fig. 11.

While after applying the proposed method, the result is re-assembling the entire 7 fragments to return to the original shape despite the loss of several fragments that have caused the emergence of a large gap. So, the Fig. 12a represents all the steps that required to reconstruct the Nabatean Drinking vessel. It was a difficult task because a lack of prior knowledge of the shape of the Nabataean Drinking cup, perhaps the bottom of vessel suffered to difficult environmental conditions, which led to crush the bottom of the cup and the fragmentation of the upper part as shown in Fig. 12b.

The algorithms have been tested on several standard fragment datasets, and the yielded results demonstrated 100% precision, because it successfully reconstructed all of the fragments and even in cases of missing fragments. Therefore, the challenge of this work is to reconstruct the objects without previous knowledge about the part that should start the assembly; this greatly helps to avoid the presence of gaps created due to missing artifact fragments. The study utilized the geometric features of the fragments as important features to reconstruct the objects by classifying their fragments using a Neural Network model.

5. Conclusions

Too many attempts made for solving the problem of reconstruction of fractured objects via digital system rather than manual assembly. Here are three great points for summarizing the advantages of this work:

Firstly, is replacing manual classification of fragments, and automate the task of classifying the fragments into groups by proposing methods that depended on color and texture characteristics.

Secondly, accurate reconstructions of the object into their original form, despite the presence of gaps, and avoid further damage to the edges of ancient fragments. Third, using a system that depends on the geometric characteristics to find matches for irregular fragments, this in turn will contribute to reduce the human resources necessary for this task.

A number of methods have been adopted to classify archaeological ceramic fragments are the color and texture of the surface information of fragments as well as has been proposed an approach to reconstruct broken 3D ceramic objects. So, the challenge for this method was to avoid the gaps which appear due to some missing fragments, this work has found the slope feature to be suitable for determining the best positions of matching pairs of fragments. Therefore, when evaluating the first method

Table 1
The comparative results of Classification the fragments between Smith et al. (2010) and the proposed method.

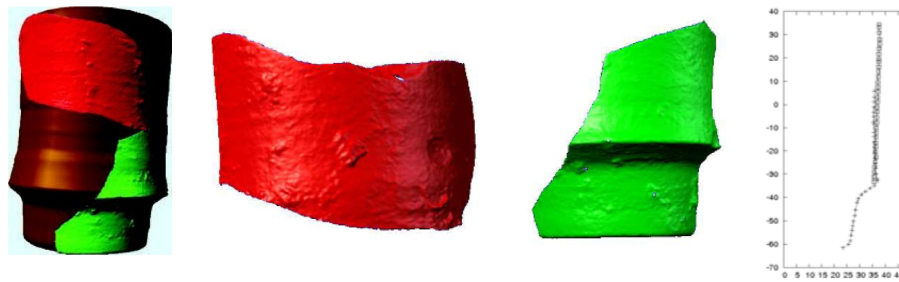| Group		Pieces	SIFT	TVG	Proposed method
Class A		9	78%	67%	100%
Class B		9	67%	56%	89%
Class C		9	78%	78%	100%
Class D		16	69%	69%	94%
Class E		2	50%	50%	100%
Class F		10	60%	70%	90%
Class G		7	71%	71%	100%
Class H		18	100%	100%	100%
All Groups		80	76%	75%	96.1%

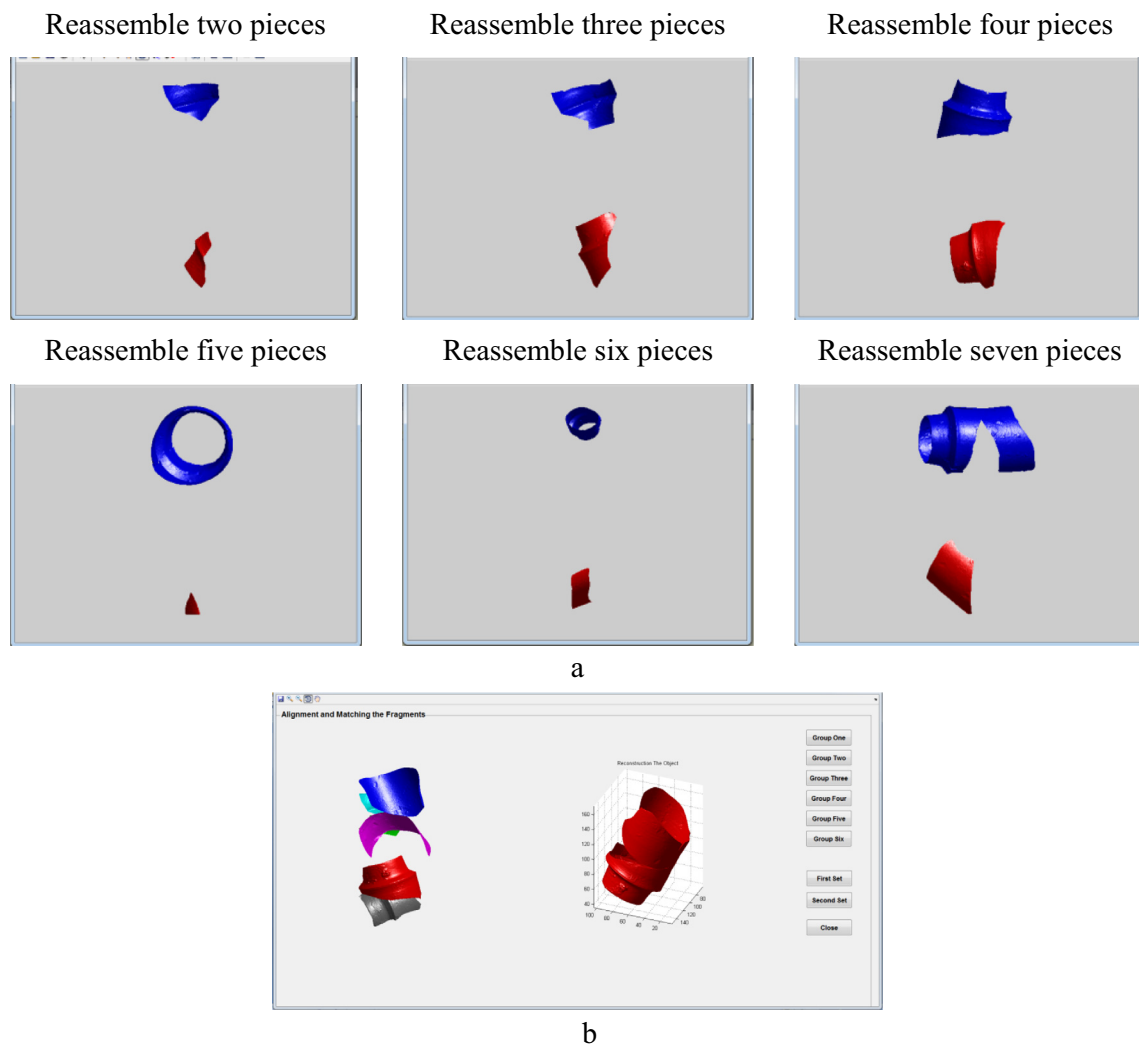**Fig. 11.** Estimating the Global Shape of Nabatean Drinking Vessel.

Fig. 12. a) Represents all the steps of reconstruct the Nabatean Drinking vessel. b) The Nabatean Drinking vessel was reconstructed using the proposed method.

for accuracy, it achieves the value of 96.1% for the classification of the fragments into similar groups. Moreover, the geometric features, especially the slope of the sub-contour with the neural network algorithm, have achieved a good accuracy to reconstruct original 3D objects. Where it is able to assemble the fragments with high efficiency. It is worth mentioning that the most challenges are creating algorithm provides a solution to align the objects through their edges and reconstruct the objects without previous knowledge about the part that should start the assembly. For further improvement, developed and modified for the robust CRAF scheme, we should depend on the angles as additional features.

References

Angelo, L. Di, Stefano, P. Di, Pane, C., 2018. An automatic method for pottery fragments analysis. Measurement 128, 138–148. Elsevier.

Beale, M.H., Hagan, M.T., Demuth, H.B., 2015. Multilayer neural network architecture. In: Neural Network Toolbox User's Guide, Matlab R2015a. Mathworks, pp. 2–9.

Belenguer, C.S., Vidal, E.V., 2012. Archaeological fragment characterization and 3d reconstruction based on projective GPU depth maps. In: IEEE 18th International Conference on VSMM, pp. 275–282.

Ceramic Sherd Database 2010. mst.cs.drexel.edu/datasets/Main/ACVA201, with permission of Drexel Computer Science and NEC Labs.

Cohen, F., Zhang, Z., Jeppson, P., 2010. Virtual reconstruction of archaeological vessels using convex hulls of surface markings. In: IEEE Computer Society Conference on Computer Vision and Pattern Recognition Workshops (CVPRW), pp. 55–61.

Duda, R.O., Hart, P.E., Stork, D.G., 2001 Chapter 6. In: Pattern Classification. second ed. Wiley- Interscience publication, pp. 10–74.

Guoguang, D., Mingquan, Z., Congli, Y., Juan, Z., Zhongke, W., Wuyang, S., 2016a. An automatic positioning algorithm for archaeological fragments. In: Proceedings of the 15th ACM SIGGRAPH Conference on Virtual-Reality Continuum and Its Applications in Industry – Volume 1 (VRCAI '16). ACM, New York, NY, USA, pp. 431–439.

Guoguang, D., Mingquan, Z., Congli, Y., Zhongke, W., Wuyang, S., 2016b. Classification and reassembly of archaeological fragments. In: Proceedings of the Symposium on VR Culture and Heritage. ACM, New York, NY, USA, pp. 67–70.

Guoguang, D., Mingquan, Z., Congli, Y., Zhongke, W., Wuyang, S., 2018a. Classifying fragments of terracotta warriors using template-based partial matching. Multimedia Tools Appl. 77 (15), 19171–21919.

Guoguang, D., Congli, Y., Mingquan, Z., Zhongke, W., Fuqing, D., 2018b. Part-in-whole matching of rigid 3D shapes using geodesic disk spectrum. Multimedia Tools Appl. 77 (15), 18881–18901.

Haralick, R.M., Shanmugan, K., Dinstein, I., 1973. Texture features for image classification. IEEE Trans. Syst., Man Cybern. 3, 610–621.

Hristov, V., Agre, G., 2013. A software system for classification of archaeological artefacts represented by 2D plans. Bulgarian Acad. Sci. Cybern. Inf. Technol. 13, 82–96.

Kampel, M., Sablatnig, R., 2000. Color classification of archaeological fragments. In: IEEE 15th International Conference on Pattern Recognition, pp. 771–774.

Karasik, A., Smilansky, U., 2011. Computerized morphological classification of ceramics. J. Archaeol. Sci. 38, 2644–2657.

Kimia, B., Aras, H., 2010. HINDSITE: a user-interactive framework for fragment assembly. In: IEEE Computer Society Conference on Computer Vision and Pattern Recognition Workshops, pp. 62–69.

Leitao, H., Stolfi, J., 2005. Measuring the information content of fracture lines. Int. J. Comput. Vision 65 (3), 163–174. Springer Science.

Lu, Y., Gardner, H., Jin, H., Liu, N., Hawkins, R., Farrington, I., 2007. Interactive reconstruction of archaeological fragments in a collaborative environment. In: IEEE 9th Biennial Conference of the Australian Pattern Recognition Society on Digital Image Computing Techniques and Applications, pp. 23–29.

Maidment, D.R., Tarboton, D., 2011. In: Computation of slope, GIS In Water Resources Class. University of Texas At Austin, pp. 1–9.

Makridis, M., Daras, P., 2012. Automatic classification of archaeological pottery sherds. ACM J. Comput. Cultural Heritage 5 (4), 1–21.

Nitecki, Z.H., 2012. In: Coordinates and vectors, Calculus in 3d geometry, Vectors. and Multivariate Calculus. Tufts University, pp. 102–114.

Ojala, T., Pietikainen, M., Harwood, D., 1996. A comparative study of texture measures with classification based on feature distributions. Pattern Recognit. 29 (1), 51–59.

Oxholm, G., Nishino, K.A., 2013. Flexible approach to reassembling thin artifacts of unknown geometry. J. Cultural Heritage 14 (1), 51–61. The Science Direct interface.

Oxholm, G., Nishino, K., 2011. Reassembling thin artifacts of unknown geometry. In: The 12th International Symposium on Virtual Reality, Archaeology and Cultural Heritage Vast, pp. 49–56.

Piccoli, C., Aparajeya, P., Papadopoulos, G.Th, Bintliff, J., Leymarie, F.F., Bes, P., Enden, M., Poblome, J., Daras, P., 2013. Towards the automatic classification of pottery sherds: two complementary approaches. In: Computer Applications and Quantative Methods In Archaeology Conference, Perth, Western Australia, pp. 1–16.

Pietikäinen, M., Hadid, A., Zhao, G., Ahonen, T., 2011. Local Binary Patterns for Still Images. In: Chapter 2 of Computer Vision Using Local Binary Patterns, Computational Imaging and Vision 40. Springer, Verlag London, pp. 13–47.

Rasheed, N.A., Nados, W.L., 2018. Object segmentation from background of 2D image. J. Univ. Babylon, Pure Appl. Sci. 26 (5), 204–215.

Rasheed, N.A., Nordin, M.J., 2015. Archaeological Fragments Classification Based on RGB Color and Texture Features. J. Theor. Appl. Inf. Technol. 76 (3), 358–365.

Smith, P., Bespalov, D., Shokoufandeh, A., Jeppson, P., 2010. Classification of archaeological ceramic fragments using texture and color descriptors. In: IEEE, Society Conference on Computer Vision and Pattern Recognition Workshops (CVPRW), pp. 49–54.

Smith, W.S., Kristof, E., 1970. Computer helps scholars re-create an egyptian temple. Natl. Geogr. Mag. 138 (5), 634–655.

Sui, Y., Willis, A.R., 2008. Using markov random fields and algebraic geometry to extract 3D symmetry properties. In: Fourth International Symposium on 3D Data Processing, Visualization and Transmission (3DPVT), Atlanta. Ga, pp. 1–8.

Toler-Franklin, C., Brown, B., Weyrich, T., Funkhouser, T., Rusinkiewicz, S., 2010. Multi-feature matching of fresco fragments. In: Proceedings of ACM SIGGRAPH. Asia. TOG Homepage, 29 (6), p. 185.

Willis, A., Cooper, D.B., 2006. Estimating a-priori unknown 3d axially symmetric surfaces from noisy measurements of their fragments. In: IEEE Third International Symposium on 3D Data Processing, Visualization, and Transmission, pp. 334–341.

Willis, A.R., Cooper, D.B., 2008. Computational reconstruction of ancient artifacts. IEEE Sig. Process. Mag. 25 (4), 65–83.

Ying, L., Gang, W., 2010. Kernel fuzzy clustering based classification of ancient-ceramic fragments. In: Proceedings of the IEEE Conference on Information Management and Engineering, pp. 348–350.

Zhou, P., Wang, K., Shui, W., 2011. Ancient porcelain shards classifications based on color features. In: Image and Graphics (ICIG), IEEE 6th International Conference on Image and Graphics, pp. 566–569.